Evaluation of Potential Impacts to Stream and Ground Water Due to Underground Coal Mining

Christopher Newman, Ph.D. Student
Zacharias Agioutantis, Professor of Mining Engineering
Gabriel Boede Jimenez Leon, Graduate Student
Department of Mining Engineering
University of Kentucky
Lexington, KY

ABSTRACT

Ground movements due to longwall mining operations have the potential to damage the hydrological balance within as well as outside the mine permit area in the form of increased surface ponding and changes to hydrogeological properties. Recently, the Office of Surface Mining, Reclamation and Enforcement has completed a public comment period on a newly proposed rule for the protection of streams and groundwater from adverse impacts of surface and underground mining operations (80 FR 44435). With increased community and regulatory focus on mining operations and their potential to adversely affect streams and groundwater, there is now a greater need for better prediction of the possible effects mining has on both surface and sub surface bodies of water.

As mining induced stress and strain within the overburden is correlated to changes in the hydrogeological properties of rock and soil, this paper investigates the evaluation of the hydrogeological system within the vicinity of an underground mining operation based on strain values calculated through a surface deformation prediction model. Through accurate modeling of the pre- and post-mining hydrogeological system, industry personnel can better depict mining induced effects on ground water flows through the overburden material aiding in the optimization underground extraction sequences while maintaining the integrity of surface and subsurface bodies of water.

INTRODUCTION

The utilization of high-recovery underground mining methods, such as longwall or high-extraction room-and-pillar operations, have the potential to cause adverse impacts to both surface and subsurface bodies of water as strata movement and deformations propagate from the mined seam through the overburden to the surface (Peng, 2008).

Previous research has indicated that mining induced strains are the most damaging to surface streams (Singh, 1992) as well as greatly affecting the integrity of subsurface bodies of water and groundwater flow conditions (Booth, 1986). On the surface, adverse effects to the stream can occur due to the development of either tensile or compressive strain in the stream bed. The development of tensile cracks along the bedrock allows for a potential loss of stream flow through developed fissures. In fact, water flow in the Cataract River of Australia ceased in 1994 as a result of mining-induced strains from longwall operations in the Bulli seam 430 meters (1320 feet) below the river gorge (McNally and Evans, 2007). On the other hand, the development of compressive strains within the rock layers can cause rupturing or buckling of the stream bed, blocking stream flow and/or diverting flow into the fractures at the base (Iannacchione et al, 2010). While these localized fractures can contribute to the loss of stream flows, given time, damaged streams have the ability to self-heal through the regeneration of near-surface aquifers as well as the sealing of mining-induced fractures with rock debris, gravel, sand, clay or other soil particles carried from upstream sources and deposited in the river bed (Waddington and Kay, 2002).

Below the surface, mining-induced strains can initiate subsidence and fracturing of the strata, causing changes to the hydraulic conductivity affecting flow paths within the overburden (Karacan and Goodman, 2009). Recently, the Office of Surface Mining Reclamation and Enforcement (OSMRE) has completed the public comment period on a newly proposed rule for the protection of streams and groundwater from the adverse impacts of surface and underground mining operations (80 FR 44435). These proposed regulations call for an increase in baseline data collection, pre- and post-mining monitoring and mitigation/restoration practices, as well as increased focus on possible mining-induced damages to the hydrogeological balance within the mine permit, which includes both surface and subsurface bodies of water. With an increase in environmental scrutiny from both local communities and regulatory agencies, this paper investigates the application of a numerical modeling approach for a more realistic evaluation of mining impacts to both surface and subsurface bodies of water.

Since the determination of the strain regime above an underground mine is integral to this investigation, the Surface Deformation Prediction Software (SDPS) will be utilized to calculate mining-induced strains at different elevations above the seam as well as on the surface. Surface strain calculations now include the effect of varying topography, while subsurface strain outputs from SPDS will be used to assess changes to the hydraulic conductivity of affected strata. An assessment of the post-mining hydrogeological system using a hypothetical case study will be presented through the application of MODFLOW, a USGS groundwater modeling software package.

This paper presents two conceptual case studies that demonstrate (a) the effect of variable surface topography to ground strains across a linear surface body (e.g., a stream) and (b) the effect of horizontal strain magnitude in the overburden on the hydraulic conductivity of different formations potentially impacted by underground mining.

BACKGROUND

The Importance of Strain in Assessing Potential Impacts to the Surface and Subsurface

The influence function method, as implemented by SDPS, for the calculation of ground deformations is a mature methodology widely used by academia, industry and regulatory agencies (Karmis et al, 2008). Through the application of this Gaussian bell-shaped influence function in SDPS, one is able to calculate horizontal displacement as a linear function of the first derivative of subsidence and horizontal strain as the first derivative of horizontal displacement. Recent advances in the SDPS package allow calculation of directional strain and ground strain along a profile as well as ground strain for random prediction points by calculating the 3D distance between neighboring surface points (Agioutantis and Karmis 2013; Agioutantis et al, 2016). The influence function formulation can actually calculate deformations at any point in 3D space and, therefore, at any point on the surface and at any elevation between the seam and the surface. This is conceptually depicted in Figure 1, where a typical horizontal strain distribution across a transverse profile line over a rectangular panels of 2 m (6.6 ft) extraction height at depths of 100 m (330 ft) and 50 m (165 ft) respectively. In addition, a horizontal strain curve is calculated at half the overburden depth. Although strain magnitudes increase as the distance from the extracted panel decreases, the inflection point of the strain curve remains above the rib.

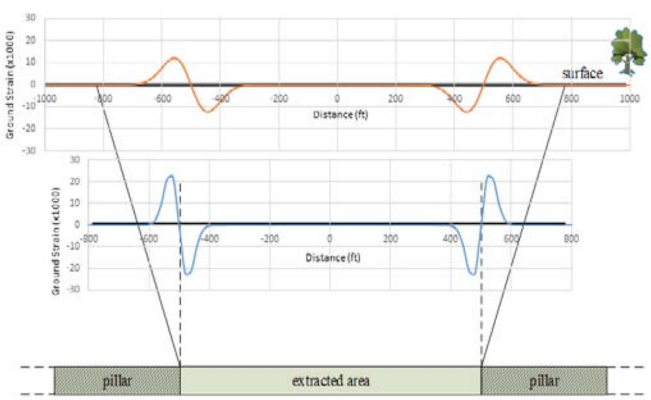

Figure 1. Distribution of horizontal strains at and below the surface over an underground extraction area.

These calculations can be easily utilized to determine potential surface impacts as discussed by Agioutantis, et al (2013) or used to derive other physical parameters for surface or groundwater modeling.

It should be emphasized, however, that further adjustments are necessary when these ground strain calculations or strain calculations within a given formation are applied to man-made structures in contact with the ground, such as buildings or pipelines (Deck and Harlaka, 2008).

Relating horizontal strain magnitudes to changes in hydraulic conductivity

While the majority of research has focused on mining-induced strain damages at the surface, strain magnitudes within the overburden can also cause detrimental impacts to the strata overlying a mined panel. Overburden strains discussed in this paper refer to the maximum horizontal strains developed within the geologic strata and, as already mentioned, can be calculated by SDPS at any point between the seam and the surface. Similar to the effects of increased strains at the surface, strains within the overburden can cause mining-induced fracturing of the overburden leading to the dewatering of both surface and subsurface bodies of water through the subsequent and large increase in hydraulic conductivity (Liu et al, 1997). While academic and industry research acknowledges that changes to the hydraulic conductivity within the overburden material can alter the groundwater system (Hawkins and Smoyer, 2011; Karacan, 2010; Booth, 2006), few studies have investigated the interaction between mining-induced strata deformations and the modifications to hydraulic conductivity.

In lieu of tedious and time-consuming groundwater monitoring regimes, groundwater flow models are often used to evaluate the impact of mining operations on the hydrogeological system through the prediction of groundwater flows and transportation processes. The three-dimensional finite-difference groundwater flow model, MODFLOW, provides users with a mathematical description of groundwater flows as well as surface-groundwater interaction through the application of Darcy's equation for fluid flow in porous material (McDonald and Harbaugh, 1988). Distributed to users through the United States Geological Survey (USGS) web site, MODFLOW is widely used within the mining industry to simulate groundwater seepage into mine openings or shafts (Zaidel et al, 2010). As with any numerical model, realistic model estimations are closely tied to input parameters; therefore, it is important that users have detailed information on site-specific geology, water quality, recharge, river locations, water levels, hydraulic parameters, etc., as well as a clear understanding of numerically embedded assumptions within the numerical modeling code such as boundary conditions, layer types, etc.

In order to accurately simulate groundwater flow paths, it is important that users can accurately quantify the hydraulic conductivity of the overburden strata material. Typically determined through borehole slug tests, hydraulic conductivity is the proportionality constant of Darcy's equations (*K*), which related the amount of flow through a unit cross-sectional area (*A*) of an aquifer under a unit gradient of hydraulic head (*Dh/ΔL*).

$$Q = KA\frac{\Delta h}{\Delta L} \tag{1}$$

In reviewing the literature, a wide range of pre- and post-mining hydraulic conductivities have been documented (as summarized in Table 1). These values have been determined through a series of in-situ borehole slug tests and/or back calculations from groundwater monitoring regimes. In reviewing the values presented in the table, all testing seems to indicate pre- and post-mining hydraulic conductivities within similar ranges. For shale materials in the overburden, the data suggests a pre-mining hydraulic conductivity in the order of 10^{-8} to 10^{-9} m/s with post-mining conductivities increasing by one or two orders of magnitude. For sandstone materials, the data suggests a typical pre-mining hydraulic conductivity values range in the order of 10^{-4} to 10^{-5} m/s with post-mining conductivities again increasing by 10-fold or 100-fold. Limestone channels within the overburden material have pre-mining hydraulic conductivities ranging in the order of 10^{-8} to 10^{-10} m/s; post-mining hydraulic conductivity were not available.

While the majority of the literature reviewed points to the same range of pre- and post-mining hydraulic conductivity for overburden strata materials, the data published by Li, et al (2015) has significantly higher conductivities for all materials. In further reviewing this publication, it is believed that the units may have been mislabeled (m/s instead of ft/d). Under this assumption, conductivity values collaborate well with the other published data. The change in hydraulic conductivity between pre- and post-mining activity is similar in magnitude change (10- to 100-fold), the data seems to suggest that there were previous impacts to the overlying strata causing such high pre-conductivity values.

According to Ouyand and Elsworth (1993), after determining the mining-induced strain field around a given panel, one can approximate the post-mining hydraulic conductivity of overburden material using the following equations:

$$K_x = K_{xo} * \left[1 + \frac{b + S(1 - R_m)}{b} \Delta\epsilon_y\right]^3 \quad (2)$$

$$K_y = K_{yo} * \left[1 + \frac{b + S(1 - R_m)}{b} \Delta\epsilon_x\right]^3 \quad (3)$$

where K_x and K_y are the post-mining hydraulic conductivities in the horizontal and vertical directions determined as a function of the pre-mining conductivity in the horizontal and vertical directions (K_{xo} and K_{yo}), the fracture aperture (b) and spacing (S), a modulus reduction ratio (Rm), and the mining-induced strains in the horizontal ($\Delta\varepsilon_x$) and vertical ($\Delta\varepsilon_y$) directions.

Thus, using the predicted, calculated or measured mining-induced strains within the overburden strata, one is able to approximate the post-mining hydraulic conductivity. Table 2 was generated using assumed values for S (1 ft or 0.33 m), b (1 mm or 0.001 m) and R_m (0.8) as the geometric parameter of Equation 3. Post-mining hydraulic conductivity increases as the strain magnitude increases by a factor of 1.2 for a strain value of 1 mm/m to a factor of 82.3 for a strain value of 50 mm/m.

Following the determination of changes in hydraulic conductivity with respect to mining-induced strains, the post-mining hydrogeological system may subsequently be defined through the application of a groundwater model (Liu et al, 1997).

A summary of the steps required are shown in the brief flowchart depicted in Figure 2. Users can input mine and surface geometry and overburden parameters into the influence function method of the SDPS package and calculate strain at any point within the overburden with respect to the defined mine layout. Taking the horizontal strain outputs from SDPS and averaging them over specific regions, one can then estimate the post-mining hydraulic conductivity with respect to Equation 3. Finally, by implementing the post-mining hydraulic conductivity values as input parameters to a hydrogeological model, one can effectively approximate the changes in groundwater flow with respect to mining-induced strains in the overburden.

CONCEPTUAL CASE STUDIES

Case Study 1: The Effect of Variable Topography on Ground Strains in the Vicinity of a Linear Water Body

The first case study discusses the effect of varying topography over a high extraction area, such as a longwall panel. The geometry of the extracted area and the transverse prediction line utilized is shown in Figure 3 (part A). The elevations of the surface points vary, as shown in Figure 3 (part B). The elevation profile presented in Figure 3b simulates a stream flowing at the bottom of a valley along the longitudinal axis of a panel. Starting from the west side of the panel, elevations gradually decrease to a minimum point that represents the stream bed and then increase again towards the eastern side of the panel. Similar work, but pertaining to a transverse stream with respect to the panel axis, was presented in Agioutantis et al (2016).

Seam (extraction) thickness is assumed at 6 ft, and the edge effect offset is taken as zero. Using a supercritical subsidence factor of 50% and default influence function parameters, the horizontal and ground strain profiles were calculated using SDPS. A discussion regarding the difference between horizontal and ground strains is available in Agioutantis and Karmis (2013) and also in Agioutantis et al (2016).

Figure 4 shows the distribution of ground strain along the transverse profile shown in Figure 3 (part B). Positive horizontal or ground strain values correspond to tension, and negative strain corresponds to compression. Two ground strain profiles are plotted: one corresponds to a surface inclination of 20°, and the other to a surface inclination of 30°. Ground strain magnitudes are comparable for both profiles. The zero strain point has slightly moved inby due to the ground strain adjustment.

Figure 5 presents the distribution of horizontal strain along two similar transverse profiles that differ only with respect to the horizontal location of the minimum elevation area. Strain magnitudes are again similar, and the slight differences can be attributed to the elevation differences between the two curves.

Figure 6 shows the distribution of ground strain along three transverse profiles; the difference between the profiles is the

Table 1. Hydraulic conductivity values in units of m/s.

	Shale		Sandstone		Limestone	Coal Seam		Aquifer	
	Pre	**Post**	**Pre**	**Post**	**Pre**	**Pre**	**Post**	**Post**	
H	7.01E-08 to 7.01E-09	7.01E-06 to 7.01E-08	7.01E-05	7.01E-03					Elsworth, et. al. (1995)
V	7.01E-08 to 7.01E-09	7.01E-07 to 7.01E-08	7.01E-05	7.01E-04					Elsworth, et. al. (1995)
H	1.13E-07 to 9.53E-08	2.89E-05 to 3.53E-07	1.14E-06 to 4.23E-08	3.42E-06 to 2.85E-05	1.76E-09	1.76E-09			Li, et. al. (2015)
H								1.65E-03 to 6.1E-06	Toran & Bradbury (1995)
V		6.1E-09 to 6.1E-11							Toran & Bradbury (1995)
H							1.74E-06 to 3.47E-07		McCoy, et. al. (1995)
H			1.0E-04 to 1.0E-05						Rapantova, et. al. (2007)
H	8.89E-09 to 2.28E-09				1.09E-08 to 5.43E-10				Karacan & Goodman (2009)

Table 2: Approximation of vertical post-mining hydraulic conductivity with respect to mining induced horizontal strain based on the formulation by Ouyand and Elsworth (1993).

ε_x	S	b	R_m	K_{yo}		K_y		K_y / K_{yo}
	[m]	[m]		[m/s]	[m/d]	[m/s]	[m/d]	
0.001	0.33	0.001	0.8	5.00E-08	4.32E-03	6.07E-08	5.25E-03	1.2
0.01	0.33	0.001	0.8	5.00E-08	4.32E-03	2.33E-07	2.01E-02	4.7
0.02	0.33	0.001	0.8	5.00E-08	4.32E-03	6.41E-07	5.54E-02	12.8
0.05	0.33	0.001	0.8	5.00E-08	4.32E-03	4.12E-06	3.56E-01	82.3

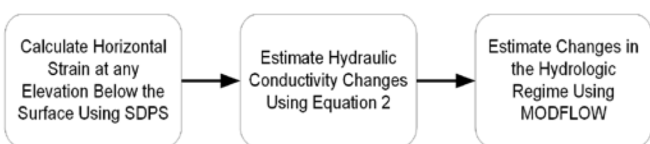

Figure 2. Flow chart for the approximation of groundwater flow with respect to mining-induced strains in the overburden material.

location of the stream bed with respect to the rib of the extracted area. The inflection point of the ground strain curve is displaced with respect to the rib, depending on the surface curve. Ground strain magnitudes are similar although the shape of the peak tensile regime and peak compressive regime may differ.

Results presented above show that the maximum ground strains expected on a stream bed can be mitigated as a function of the relative location of the stream axis to the rib of the excavation.

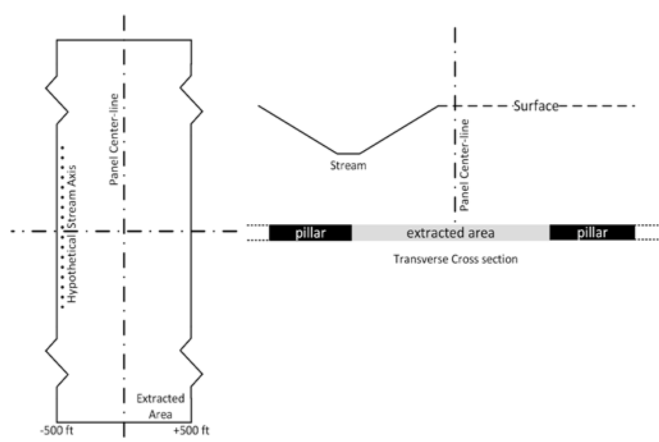

Figure 3. (a) Plan view and (b) section view of modeled area.

Case Study 2: The Effect of Horizontal Strain on Groundwater Flow

To evaluate the effect of mining-induced strains on the hydrogeological system, a conceptual model containing a subsurface aquifer overlying an active longwall panel was developed using MODFLOW. With an excavation height of 2 m, the caving zone, as defined by Peng and Chiang (1984), extends 20 m (5-10 times the seam thickness) from the coal seam into the overburden strata. As shown in Figure 7, the subsurface aquifer is therefore located in the fractured zone (30-50 times the seam thickness). In order to evaluate the effect of mining-induced strains on groundwater flow conditions, pre- and post-mining groundwater models were developed simulating water flows through a simplistic three-dimensional block 1380 m (4528 ft) wide (138 elements), 2000 m (6562 ft) long (200 elements) and 100 m (328 ft) deep. Each model has been developed such that it simulates water flow over a year, given 12 (time) stress periods each spanning 30 days.

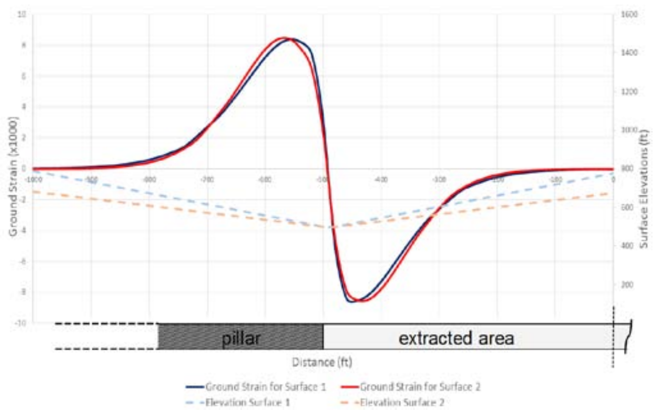

Figure 4. Ground strain profiles on a transverse line above a longwall panel. Surface 1 corresponds to 30 degrees, and Surface 2 to 20 degrees.

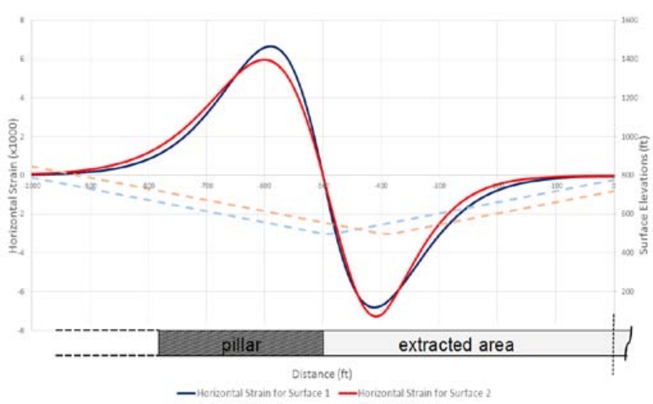

Figure 5. Horizontal strain profiles on a transverse line above a longwall panel. Surfaces 1 and 2 are both sloping 30 degrees to the horizontal, but with a different location of the minimum elevation.

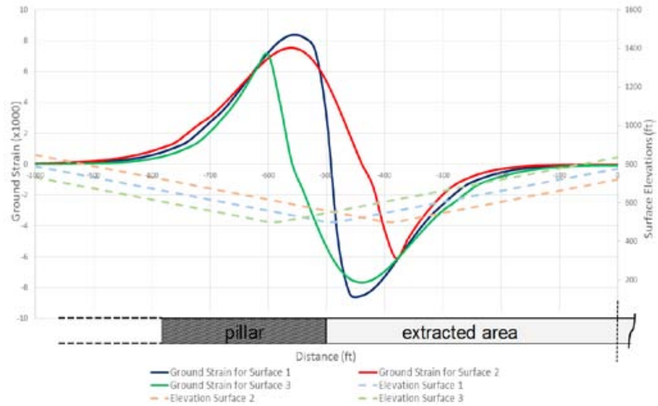

Figure 6. Ground strain profiles on a transverse line above a longwall panel. The stream bed in Surface 1 is close to the rib, the stream bed in Surface 2 is inby and in Surface 3 it is outby.

Each model is comprised of four layers (Figure 8) corresponding to four stratified geological formations. Their respective geometric as well as pre- and post-mining hydraulic properties are given in Table 3. Layer 1 was defined as an unconfined shale formation 40 m (131 ft) thick with a hydraulic conductivity of 0.0864 m/d (1.00E-06 m/s) in both the horizontal and vertical directions as interpreted from the literature. Layer 2 was defined with as an unconfined aquifer (sandstone) with variable transmissivity layer type that is 20 m (66 ft) thick with a pre-mining vertical and horizontal hydraulic conductivity of 8.64 m/d (1.00E-04 m/s) and a post-mining vertical and horizontal conductivity of 86.4 m/d (1.00E-03 m/s) correlating to a strain value of 0.01723. Since Layer 2 represents an unconfined water-bearing sandstone aquifer, an initial head of 60 m was defined for Layer 2 while Layers 1, 3, and 4 of the model were defined with initial heads of zero.

Layer 3 was defined as a confined shale formation 40 m (131 ft) thick with a pre-mining vertical and horizontal conductivity of 0.0866 m/d (1.00E-06 m/s) and a post-mining vertical and horizontal conductivity of 0.864 m/d (1.00E-05 m/s), correlating to a strain value of 0.01723. Layer 4 was defined as a confined coal seam which is 2 m (6.4 ft) thick with a pre-mining vertical and horizontal conductivity of 0.864 m/d (1.00E-05 m/s) and a post-mining vertical and horizontal conductivity of 8.64 m/d (1.00E-04 m/s).

As MODFLOW operates with differences in head and/or elevation, an arbitrary datum of zero elevation was assumed to lie at the top of Layer 4 such that the cumulative thickness of layers 1-3 represents the overburden depth over the coal seam. All layers within this model were defined with default values for specific storage (0.0001 / m) and specific yield (0.25). Post-mining hydraulic conductivities were defined in the areas of mining disturbance, and their magnitude was estimated based on horizontal strains determined by the influence function method of the SDPS package (Table 3). Recharge of the groundwater system due to precipitation was not considered in this model, nor was the removal of water from the system with respect to plant transpiration or evaporation.

Table 3: Input parameters for MODFLOW models.

Layer	Thickness	Hyd. Head	Pre-mining		Horiz. Strain	Post-mining		Change in Hyd. Cond.	Comments
	[m]	[m]	[m/s]	[m/day]		[m/s]	[m/day]		
Layer 1	40	0	1.00E-06	0.0864	0.00	1.00E-06	0.0864	1	Overburden assumer impermeable
Layer 2	20	60	1.00E-04	8.64	0.0172	1.00E-03	86.4	10	Aquifer assumer unconfined
Layer 3	40	0	1.00E-06	0.0864	0.0172	1.00E-05	0.864	10	Overburden assumer impermeable
Layer 4	2	0	1.00E-05	0.864	0.0172	1.00E-04	8.64	10	Coal Seam

As shown in Figure 8 and Figure 9, two boundary conditions have been applied to the sandstone aquifer (Layer 2) for both pre- and post-mining groundwater models. A general head boundary with a conductance of 34.25 m^2/d (3.96E-04 m^2/s) has been defined on the eastern edge of the aquifer, while a drain with a conductance of 34.25 m^2/d (3.96E-04 m^2/s) has been defined along the western boundary of the aquifer. In defining these boundary conditions, water flow through the aquifer can be simulated by the model. In order to simulate the post-mining flow of groundwater into the mine with respect to the excavation of coal by the longwall, drains with a conductance of 0.5 m^2/d (6.00E-06 m^2/s) have been defined for element 46 to 92 in Layer 4, as shown in Figure 9.

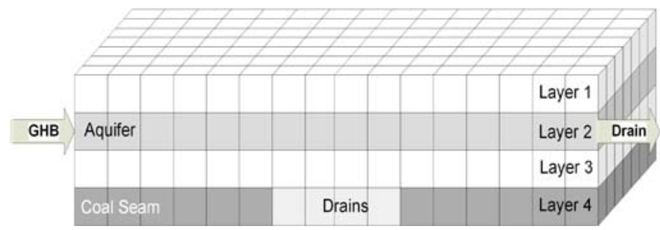

Figure 9. Post-mining groundwater model (not to scale).

RESULTS & DISCUSSION

Comparing the MODFLOW results of the pre- and post-mining head of the aquifer for this hypothetical case study, one is able to evaluate the impact of mining-induced strains on groundwater conditions. Before mining occurs, the water level within the aquifer gradually decreases from an initial head of 60 m to a head of 51 m across the simulated area, as represented by the blue line shown in the cross-section presented in Figure 10. Note that unconfined aquifers may show either a head decrease or a constant head along a specific length.

These results are then compared to that of the post-mining water levels within the aquifer. In these cases, groundwater flow simulations start after all mining has been completed, while pumping (water loss) at mine level continues. Here, one finds that the increase in hydraulic conductivity with respect to mining-induced strains in the overburden result in the dewatering of the aquifer in the area directly overlaying the mined-out panel. The simulation is performed for periods of one, two, and three years for a constant water removal rate.

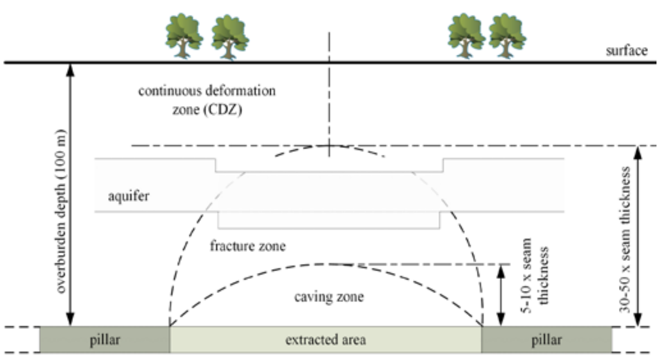

Figure 7. Aquifer location with respect to the fracture and caving zones (adapted from Peng, 2008).

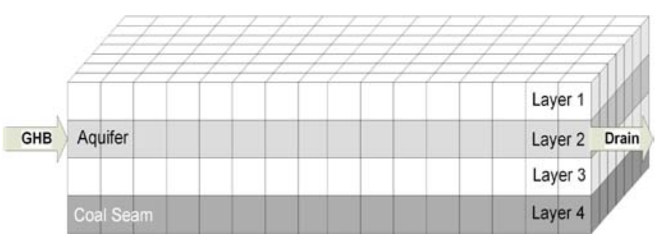

Figure 8. Pre-mining groundwater model (not to scale).

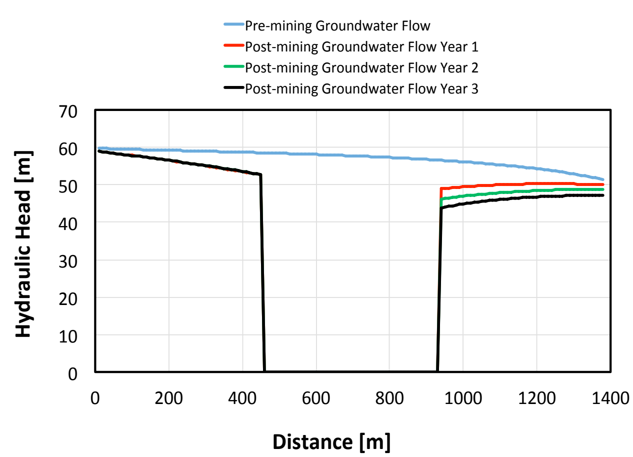

Figure 10. The effect of mining on groundwater flow through an aquifer.

As shown in Figure 10, for all simulated time periods, the hydraulic head within the aquifer gradually decreases as it approaches the longwall panel. In the overburden area directly above the longwall panel, water within the aquifer is lost to the lower geologic layers due to the mining-induced increase in hydraulic conductivity for years one, two, and three. On the eastern side of the longwall panel, in the area of non-impacted overburden material, the hydraulic head gradually decreases from the eastern boundary to the eastern edge of the gob panel as groundwater flows into the mine workings. As simulation time increases to years two and three, the water level at the eastern side tends to decrease as pumping continues and there is no recharge applied to the model. These graphs are indicative of aquifer behavior since simulation results depend on model assumptions regarding formation permeability and storativity, as well water input and outputs. Furthermore, once mining operations cease and aquifer water is not removed from the system, simulations show that the aquifer will recover to its original levels.

This is similar to observed downstream waters level recovery in surface streams. (Tieman and Raunch, 1992). Mining-induced surface cracks can potentially drain streams in areas above underground longwall panels. The water is diverted through these cracks into subsurface aquifers. Given time, these aquifers will become full and force water back to the surface downstream from where the original water loss occurred.

SUMMARY AND CONCLUSION

Increases in environmental scrutiny from community and regulatory agencies have created significant obstacles for mining companies to obtain mining and reclamation permits (Booth, 2006). Currently, the Office of Surface Mining Reclamation and Enforcement (OSMRE) is looking to impose new regulations in 2016 for the protection of streams and groundwater from adverse impacts of surface and underground mining operations (80 FR 44435), which could possibly sterilize large amounts of coal reserves.

This paper examines the implementation of a general methodology for operations personnel to evaluate mining-induced impacts on surface and subsurface bodies of water. Through the utilization of the influence function formulation in SDPS, one is able to predict mining-induced ground deformations at any point in the three-dimensional space and, therefore, at any point along the surface topography or at any elevation within the overburden strata.

A hypothetical case study simulating a stream in a hill/valley system is utilized for calculating the distribution of ground strain along linear surface water bodies under simple geometrical considerations. Calculations indicate that the maximum ground strains expected on a stream bed can be mitigated as a function of the relative location of the stream axis to the rib of the excavation. More work needs to be done for quantifying the effect of stream orientation, overburden topography to panel orientation and edge effect offset.

A second hypothetical case study was investigated where subsurface strain outputs from SDPS were used in the assessment of mining-induced changes to the hydraulic conductivity of the overburden strata and, therefore, changes to the hydrogeological system above a high-extraction area. Results show that in overburden areas disturbed by underground mining operations, groundwater levels at an aquifer will gradually decrease while water is removed from the underground working through pumping or other means. When water outflows at mine level cease then the aquifer present in the overburden will rebound. While the results presented in this approach point to a promising methodology for the evaluation of mining-induced impacts on subsurface bodies of water, further research is needed for validating hydraulic conductivity changes and water head distribution above high-extraction areas.

ACKNOWLEDGEMENT

This study is sponsored by the Appalachian Research Initiative for Environmental Science (ARIES). The views, opinions and recommendations expressed in this paper are solely those of the authors and do not imply any endorsement by ARIES employees or other ARIES-affiliated researchers. The authors would also like to thank the reviewers of this paper for their diligence in technically reviewing this work.

REFERENCES

Agioutantis, Z., Newman, C., Böde Jimenez Leon, G., and Karmis, M. (2016). “Minimizing impacts on streams due to underground mining by predicting surface ground movements.” *Mining Engineering*, 68(3), 28-37.

Agioutantis, Z. and Karmis, M. (2013). “Recent Developments on Surface Ground Strain Calculations due to Underground Mining in Appalachia.” In: *Proceedings, 32nd International Conference on Ground Control in Mining*, 30 July–1 August 2013, Morgantown, West Virginia, 214-219.

Agioutantis, Z., Karmis M. and Kirby, L. (2013). “Application of Subsidence Prediction Methodologies for Sizing Barrier Pillars for Stream Protection in Appalachia.” In: *Proceedings, Symposium on Environmental Considerations in Energy Production*, J.R. Craynon, SME, ed. April 14-18, Charleston, West Virginia, 319-335.

Booth, C.J. (1986). “Strata-movement concepts and the hydrogeological impact of underground coal mining.” *Ground Water*, 24(4), 507-515.

Booth, C.J. (2006). “Groundwater as an environmental constraint of longwall coal mining.” *Materials and Geoenvironment*, 50(1), 49-52.

Deck, O. and A. Harlaka, (2008), Study of Soil-Structure Interaction Phenomena Within Mining Subsidence Areas, Post-Mining 2008, February 6-8, Nancy, France

Hawkins, J. and Smoyer, J.J. (2011). “Hydrologic Impacts of Multiple-Seam Underground and Surface Mining: A Northern Appalachia Example.” *Mine Water and the Environment*, 30(4), 263-273.

Iannacchione, A., Tonsor, S., Witkowski, M., Benner, J., Hale, A. and Shendge, M. (2010). *The effects of subsidence resulting from underground bituminous coal mining on surface* *structures and features and on water resources: 3rd ACT 54 five-year report*. University of Pittsburgh.

Karacan, C.Ö. (2010). "Prediction of porosity and permeability of caved zone in longwall gobs." *Transport in Porous Media*, 82(2), 13-439.

Karacan, C.Ö. and Goodman, G. (2009). "Hydraulic conductivity changes and influencing factors in longwall overburden determined by slug tests in gob gas ventholes." *International Journal of Rock Mechanics and Mining Sciences*, 46(7), 1162-1174.

Karmis, M., Agioutantis Z., and Andrews, K. (2008). "Enhancing Mine Subsidence Prediction and Control Methodologies." In: *Proceedings, 27th International Conference on Ground Control in Mining*, July 29-31, 2008, Morgantown, West Virginia, 131-136.

Li, Y., Peng, S. S., and Zhang, J. (2015). "Impact of longwall mining on groundwater above the longwall panel in shallow coal seams." *Journal of Rock Mechanics and Geotechnical Engineering*, 7(3), 298-305.

Liu, J., Elsworth, D., and Matetic, R.J. (1997). "Evaluation of the post-mining groundwater regime following longwall mining." *Hydrological Processes*, 11(15), 1945-1961.

McCoy, K. J., Donovan, J. J., and Leavitt, B. R. (2004). "Estimation of Hydraulic Conductivity of Coal Mine Barriers, Pittsburgh Coal, Northern West Virginia, 1992-2000." In: *Proceedings, 25th West Virginia Surface Mine Drainage Task Force*, April 18-24, 2004, Lexington, Kentucky, 1218-1226.

McDonald, M. G., and A. W. Harbaugh (1988). "A modular three-dimensional finite-differences groundwater flow model." In: *Techniques of Water-Resources Investigations*. Reston, Virginia: U.S. Geological Survey.

McNally, G. and Evans, R. (2007). Impacts of longwall mining on surface water and ground water, southern coalfield NSW. NSW Department of Environment and Climate Change. eWater Cooperative Research Center, Australia.

Ouyang, Z. and Elsworth, D. (1993). "Evaluation of groundwater flow into mined panels." *International Journal of Rock Mechanics and Mining Sciences*, 30(2), 71-79.

Peng, S.S. (2008). *Coal Mine Ground Control*, 3rd Ed., West Virginia University, Morgantown, West Virginia, 750p.

Peng, S.S. and Chiang, H.S. (1984). *Longwall mining*. Wiley, New York, 708p.

Rapantova, N., Grmela, A., Vojtek, D., Halir, J., and Michalek, B. (2007). "Ground water flow modeling applications in mining hydrogeology." *Mine Water and the Environment*, 26(4), 264-270.

Singh, M.M. (1992). Mine Subsidence, Section 10.6, SME Mining Engineering Handbook, 2nd Ed., SME, Littleton, Colorado, 967-971.

Tieman, G. and Rauch, H. (1992). "Study of dewatering effects at a longwall mine in northern West Virginia." *3rd Workshop on Surface Subsidence due to Underground Mining*, Morgantown, West Virginia, 214-221.

Toran, L., and Bradbury, K. R. (1988). "Groundwater Flow Model of Drawdown and Recovery Near an Underground Mine." *Ground Water*, 26(6), 724-733.

Waddington, A. A, and Kay, D. R. (2002). "Research into the impacts of mine subsidence on the strata and hydrology of river valleys and development of management guidelines for undermining cliffs, gorges, and river systems – Stage 2." Australian Coal Association Research Program (ACARP). ACARP research report project C9067. Brisbane, Australia, 278p.

Zaidel, J., Markham, B., and Bleiker, D. (2010). "Simulating seepage into mine shafts and tunnels with MODFLOW." *Ground Water*, 48(3), 390-400.